Effect of PEG and mPEG–anthracene on tRNA aggregation and particle formation

ARTICLE *in* BIOMACROMOLECULES · DECEMBER 2011

Impact Factor: 5.75 · DOI: 10.1021/bm2016515 · Source: PubMed

5 AUTHORS, INCLUDING:

Emilie Froehlich
Université du Québec à Trois-Rivières
7 PUBLICATIONS **366** CITATIONS
SEE PROFILE

Laurent Kreplak
Dalhousie University
83 PUBLICATIONS **2,154** CITATIONS
SEE PROFILE

Heidar-Ali Tajmir-Riahi
Université du Québec à Trois-Rivières
261 PUBLICATIONS **6,598** CITATIONS
SEE PROFILE

Article

pubs.acs.org/Biomac

Effect of PEG and mPEG-Anthracene on tRNA Aggregation and Particle Formation

E. Froehlich,[†] J. S. Mandeville,[†] D. Arnold,[‡] L. Kreplak,[‡] and H. A. Tajmir-Riahi[†,*]

[†]Department of Chemistry-Biology, University of Québec at Trois-Rivières, C.P. 500, Trois-Rivières (Québec), Canada G9A 5H7

[‡]Department of Physics, Sir James Dunn Building, Dalhousie University, Lord Dalhousie Drive, Halifax, Canada NS B3H 3J5

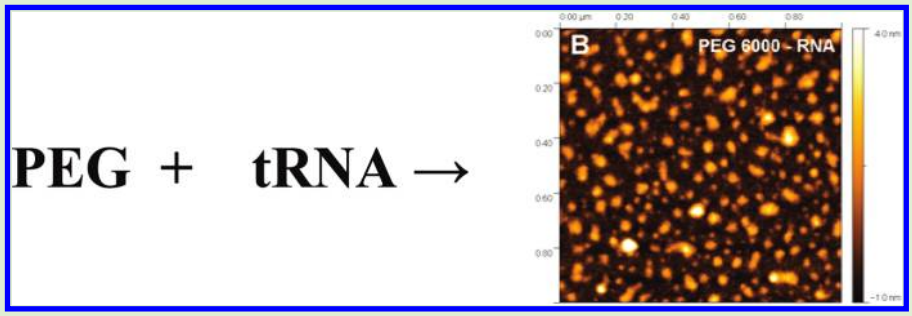

ABSTRACT: Poly(ethylene glycol) (PEG) and its derivatives are synthetic polymers with major applications in gene and drug delivery systems. Synthetic polymers are also used to transport miRNA and siRNA in vitro. We studied the interaction of tRNA with several PEGs of different compositions, such as PEG 3350, PEG 6000, and mPEG-anthracene under physiological conditions. FTIR, UV−visible, CD, and fluorescence spectroscopic methods as well as atomic force microscopy (AFM) were used to analyze the PEG binding mode, the binding constant, and the effects of polymer complexation on tRNA stability, aggregation, and particle formation. Structural analysis showed that PEG-tRNA interaction occurs via RNA bases and the backbone phosphate group with both hydrophilic and hydrophobic contacts. The overall binding constants of $K_{\text{PEG 3350-tRNA}}$= 1.9 (±0.5) × 10^4 M^{-1}, $K_{\text{PEG 6000-tRNA}}$ = 8.9 (±1) × 10^4 M^{-1}, and $K_{\text{mPEG-anthracene}}$= 1.2 (±0.40) × 10^3 M^{-1} show stronger polymer−RNA complexation by PEG 6000 and by PEG 3350 than the mPEG-anthracene. AFM imaging showed that PEG complexes contain on average one tRNA with PEG 3350, five tRNA with PEG 6000, and ten tRNA molecules with mPEG-anthracene. tRNA aggregation and particle formation occurred at high polymer concentrations, whereas it remains in A-family structure.

INTRODUCTION

Synthetic polymers play a major role in drug and gene delivery.[1−3] Among synthetic polymers, poly(ethylene glycol) and its derivatives show potential applications in gene and drug delivery due to their solubility, nontoxicity, and biocompatibility.[4,5] It has been shown that PEG induces significant changes in DNA solubility and structure under given conditions.[6] DNA concentration, pH, ionic strength of the solution, and the presence of divalent metal ions have been shown to impact PEG-DNA precipitation.[6] PEGylation of synthetic polymers such as dendrimers is shown to reduce toxicity and increase biocompatibility and DNA transfection.[4,5,7] Similarly, the effect of PEGylation on the toxicity and permeability of biopolymers such as chitosan has been recently reported.[8,9] Whereas major attention has been focused on polymer−DNA complexes because of their applications in gene delivery, little is known about polymer−RNA interaction. Synthetic polymers can transport miRNA and siRNA in vitro.[10−12] The interaction of dendrimers with tRNA has been recently reported.[13] Even though the interactions of PEGylated dendrimers with DNA, RNA, and protein are well-characterized,[13−16] detailed structural analysis of PEG and mPEG derivatives complexes with RNA is not known. Therefore, it was of interest to study the interaction of PEGs and mPEG-derivatives with tRNA, using spectroscopic methods and AFM imaging.

Fluorescence quenching has been used as a technique for quantifying the binding affinities of macromolecules with ligands.[17] Fluorescence quenching is the decrease of the quantum yield of fluorescence from a fluorophore, induced by a variety of molecular interactions with quencher molecule. Therefore, it is possible to use quenching of the mPEG-anthracene as a tool to study the interaction of PEG with tRNA, in an attempt to characterize the nature of polymer-RNA complexation.

We report the interaction of tRNA with PEG 3350, PEG 6000, and mPEG-anthracene under physiological conditions, using constant RNA concentration and various polymer contents. FTIR, CD, and UV−visible spectroscopic methods as well as AFM were used to determine the polymer binding site, binding constant, tRNA aggregation, and particle formation in the presence of PEG and its derivatives. Our spectroscopic study provides a major structural analysis of

Received: November 22, 2011
Revised: December 5, 2011
Published: December 17, 2011

PEG-tRNA binding, which helps elucidate the nature of this biochemically important interaction in vitro.

EXPERIMENTAL SECTION

Materials. Transfer RNA from Baker's yeast was purchased from Sigma Chemical and used as supplied. The A_{260}/A_{280} ratio of tRNA was 2.2, indicating that the tRNA was sufficiently free from proteins.[18] PEG 3350 and PEG 6000 were purchased form Aldrich Chemical and used as supplied. mPEG-anthracene was purchased from Polymer Source (Quebec). Other chemicals were of reagent grades and used without further purification.

Preparation of Stock Solution. Sodium-tRNA was dissolved to 1% w/w (10 mg/mL) in 10 mL of Tris-HCl (pH 7.3) at 5 °C for 24 h with occasional stirring to ensure the formation of a homogeneous solution. The final concentration of the stock tRNA solution was determined spectrophotometrically at 260 nm by using molar extinction coefficient of 6600 cm^{-1} M^{-1} (expressed as molarity of phosphate groups).[19,20] The UV absorbance at 260 nm of a diluted solution (40 μM) of tRNA used in our experiments was measured to be 0.25 (path length was 1 cm), and the final concentration of the stock tRNA solution was calculated to be 25 mM in tRNA phosphate. The appropriate amount of PEG and its derivatives (0.25 to 2 mM) was prepared in distilled water and diluted in Tris-HCl. The PEG solution was then added dropwise to the tRNA solution.

FTIR Spectroscopy. Infrared spectra were recorded on a FTIR spectrometer (Impact 420 model), equipped with DTGS (deuterated triglycine sulfate) detector and KBr beam splitter, using AgBr windows. Spectra were collected after 2 h of incubation of PEG with tRNA solution and measured in triplicate. Interferograms were accumulated over the spectral range 4000−400 cm^{-1} with a nominal resolution of 2 cm^{-1} and a minimum of 100 scans. The polymer concentrations used in infrared were 0.125, 0.25, 0.5, and 1 mM with final tRNA content of 12.5 mM (P). The water subtraction was carried out using distilled water as a reference at pH 7.3.[21] A good water subtraction was achieved as shown by a flat baseline around 2200 cm^{-1}, where the water combination mode is located. The difference spectra [(tRNA solution + PEG) − (tRNA solution)] were obtained, using the sharp tRNA band at 968 cm^{-1} as internal reference. This band, which is due to deoxyribose C−C stretching vibration, exhibits no spectral changes (shifting or intensity variation) in the PEG-RNA complexes and is canceled out upon spectral subtraction. The spectra are smoothed with Savitzky−Golay procedure.[21]

The plots of the relative intensity (R) of several peaks of tRNA in-plane vibrations related to A-U, G-C base pairs and the PO_2^- stretching vibrations such as 1698 (guanine), 1660 (uracil), 1609 (adenine), 1485 (cytosine), and 1241 (PO_2^- asymmetric) versus polymer concentrations were obtained after peak normalization using

$$R_i = \frac{I_i}{I_{968}} \tag{1}$$

where I_i is the intensity of absorption peak for pure tRNA and tRNA in the complex with i concentration of polymer and I_{968} is the intensity of the 968 cm^{-1} peak (internal reference).[22]

CD Spectroscopy. Spectra of tRNA and PEG-tRNA adducts were recorded at pH 7.3 with a Jasco J-720 spectropolarimeter. A quartz cell with a path length of 0.01 cm was used for measurements in the far-UV region (200−320 nm). Six scans were accumulated at a scan speed of 50 nm/min, with data being collected at every nanometer from 200 to 320 nm. Sample temperature was maintained at 25 °C using a Neslab RTE-111 circulating water bath connected to the water-jacketed quartz cuvette. Spectra were corrected for buffer signal, and conversion to the Mol CD ($\Delta\varepsilon$) was performed with the Jasco Standard Analysis software. The polymer concentrations used were 0.125, 0.25, 0.5, and 1 mM with final tRNA content of 2.5 mM.

Absorption Spectroscopy. The absorption spectra were recorded on a Perkin-Elmer Lambda 40 spectrophotometer with a slit of 2 nm and scan speed of 240 nm min^{-1}. Quartz cuvettes of 1 cm were used. The absorbance assessments were performed at pH 7.3 by keeping the concentration of tRNA constant (125 μM) while varying the concentration of PEG (5 to 80 μM).

To calculate the binding constant (k) for polymer−tRNA complexes, it is assumed that the interaction between the ligand L and the substrate S is 1:1; for this reason, a single complex SL (1:1) is formed.[23] It was also assumed that the sites (and all the binding sites) are independent; finally, the Beer's law is followed by all species. A wavelength is selected at which the molar absorptivity ε_S (molar absorptivity of the substrate) and ε_{11} (molar absorptivity of the complex) are different. Then, at total concentration S_t of the substrate, in the absence of ligand the light path length is b = 1 cm, and the solution absorbance is

$$A_o = \varepsilon_S b S_t \tag{2}$$

In the presence of ligand at total concentration L_t, the absorbance of a solution containing the same total substrate concentration is

$$A_L = \varepsilon_S b[S] + \varepsilon_L b[L] + \varepsilon_{11} b[SL] \tag{3}$$

where [S] is the concentration of the uncomplexed substrate, [L] is the concentration of the uncomplexed ligand, and [SL] is the concentration of the complex, which combined with the mass balance on S and L, gives

$$A_L = \varepsilon_S b S_t + \varepsilon_L b L_t + \Delta\varepsilon_{11} b[SL] \tag{4}$$

where $\Delta\varepsilon_{11} = \varepsilon_{11} - \varepsilon_S - \varepsilon_L$ (ε_L molar absorptivity of the ligand). By measuring the solution absorbance against a reference containing ligand at the same total concentration L_t, the measured absorbance becomes

$$A = \varepsilon_S b S_t + \Delta\varepsilon_{11} b[SL] \tag{5}$$

Combining eq 4 with the stability constant definition K_{11} = [SL]/[S][L], gives

$$\Delta A = K_{11}\Delta\varepsilon_{11} b[S][L] \tag{6}$$

where $\Delta A = A - A_o$. From the mass balance expression S_t = [S] + [SL], we get [S] = $S_t/(1 + K_{11}[L])$, which is eq 5, giving eq 6 at the relationship between the observed absorbance change per centimeter and the system variables and parameters.

$$\frac{\Delta A}{b} = \frac{S_t K_{11}\Delta\varepsilon_{11}[L]}{1 + K_{11}[L]} \tag{7}$$

Equation 6 is the binding isotherm, which shows the hyperbolic dependence on free ligand concentration.

The double-reciprocal form of plotting the rectangular hyperbola $(1/y) = (f/d)\cdot(1/x) + (e/d)$ is based on the linearization of eq 6 according to the following equation

$$\frac{b}{\Delta A} = \frac{1}{S_t K_{11}\Delta\varepsilon_{11}[L]} + \frac{1}{S_t\Delta\varepsilon_{11}} \tag{8}$$

Therefore, the double reciprocal plot of $1/\Delta A$ versus $1/[L]$ is linear, and the binding constant can be estimated by the following equation

$$K_{11} = \frac{\text{intercept}}{\text{slope}} \tag{9}$$

Fluorescence Spectroscopy. Fluorometric experiments were carried out on a Varian Cary Eclipse. Solution of mPEG-anthracene (80 μM) was prepared at 25 ± 1 °C. Various solutions of tRNA (5 to 100 μM) in 10 mM Tris-HCl (pH. 7.4) were also prepared at 25 ± 1 °C. The fluorescence spectra were recorded at λ_{exc} = 330−350 nm and λ_{em} 390−450 nm related to anthracene fluoropore.[24] The intensity at 420 nm was used to calculate the binding constant (K) for mPEG-anthracene-tRNA adducts. Similar method has been used to calculate the binding constant of retinol and retinoic acid to tRNA.[25]

On the assumption that there are (n) substantive binding sites for quencher (Q) on protein (B), the quenching reaction can be shown as follows

$$nQ + B \Leftrightarrow Q_nB \tag{10}$$

dx.doi.org/10.1021/bm2016515 | Biomacromolecules 2012, 13, 282−287

The binding constant (K_A), can be calculated as

$$K_A = [Q_nB]/[Q]^n[B] \quad (11)$$

where, [Q] and [B] are the quencher and polymer concentration, respectively, $[Q_nB]$ is the concentration of nonfluorescent fluorophore-quencher complex, and $[B_0]$ gives total polymer concentration

$$[Q_nB] = [B_0] - [B] \quad (12)$$

$$K_A = ([B_0] - [B])/[Q]^n[B] \quad (13)$$

The fluorescence intensity is proportional to the polymer concentration as described

$$[B]/[B_0] \propto F/F_0 \quad (14)$$

Results from fluorescence measurements can be used to estimate the binding constant of polymer−RNA complex. From eq 13

$$\log[(F_0 - F)/F] = \log K_A + n \log[Q] \quad (15)$$

The accessible fluorophore fraction (f) can be calculated by modified Stern−Volmer equation

$$F_0/(F_0 - F) = 1/fK[Q] + 1/f \quad (16)$$

where F_0 is the initial fluorescence intensity and F is the fluorescence intensities, in the presence of quenching agent (or interacting molecule). K is the Stern−Volmer quenching constant, [Q] is the molar concentration of quencher, and f is the fraction of accessible fluorophore to a polar quencher, which indicates the fractional fluorescence contribution of the total emission for an interaction with a hydrophobic quencher.[17] The plot of $F_0/(F_0 - F)$ versus $1/[Q]$ yields f^{-1} as the intercept on y axis and $(fK)^{-1}$ as the slope. Therefore, the ratio of the ordinate and the slope gives K.

Atomic Force Microscopy. PEG-tRNA complexes at a ratio of 1:1 and final tRNA concentration of 0.1 mM were prepared in 5 mL of Tris-HCl (pH 7.4). The solutions were prepared and used undiluted or diluted further in ultrapure water. For each sample, 30 μL of aliquot was adsorbed for 2 min on freshly cleaved muscovite mica. The surface was rinsed thoroughly with 10 mL of ultrapure water and dried with Argon. AFM imaging was performed in acoustic mode at a scanning speed of 1 Hz with a Pico-AFM (Molecular Imaging, Phoenix, AZ) using high-frequency (300 kHz) silicon cantilevers with a tip radius of 10 nm (TESP, Veeco, Santa Barbara, CA). Images were treated using the software Gwyddion (http://gwyddion.net/).

RESULTS AND DISCUSSION

FTIR Spectra of PEG-tRNA Complexes. The IR spectral features for PEG-tRNA complexes are presented in Figures 1 and 2.

PEG-Base Binding. Evidence of PEG-base binding comes from the spectral changes observed for the free tRNA upon complexation. At low polymer concentration 0.125 mM, no major shifting of the guanine band at 1698, uracil band at 1660 cm^{-1}, and adenine band 1609 cm^{-1} [21,22,26−31] was observed upon polymer complexation. However, an increase in intensity for the bands at 1698 (guanine), 1660 (uracil), and 1609 cm^{-1} (adenine) was observed in the spectra of the PEG-tRNA adducts (Figures 1 and 2A−C, diff., 0.125 mM). The observed spectral changes are due to a minor polymer−RNA interaction at low PEG concentration. At higher polymer concentrations, the guanine band at 1698 cm^{-1} shifted to a higher frequency at 1700 (PEG 3350), 1701 (PEG 6000), and 1699 cm^{-1} (mPEG-anthracene), upon tRNA complexation (Figure 1A−C, complexes 1 mM). The uracil band at 1660 shifted to a lower frequency at 1655−1654, and the adenine band at 1609 appeared at 1607 cm^{-1} in the spectra of the polymer−tRNA complexes (Figure 1A−C, complexes 1 mM). The spectral changes observed for guanine, uracil, and adenine bands are indicative of polymer bindings to guanine and adenine N7

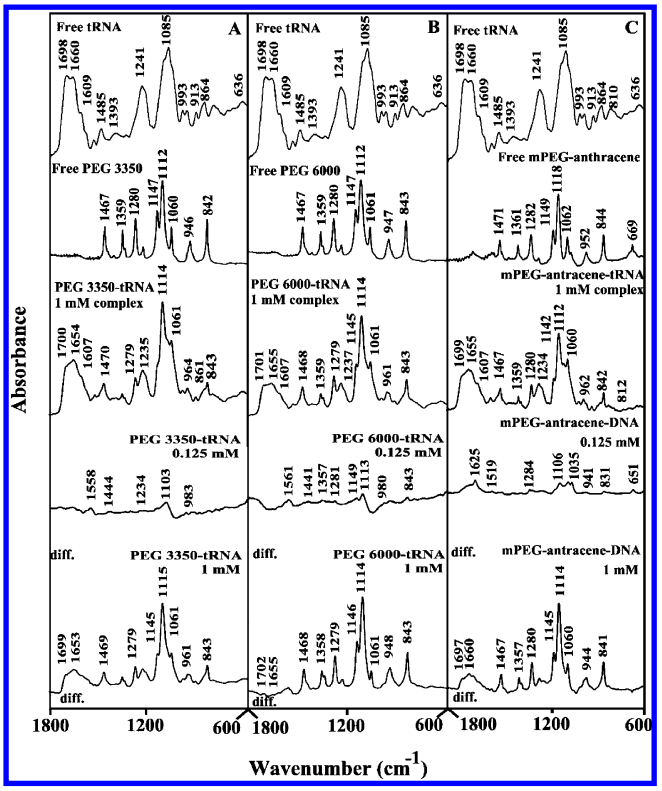

Figure 1. FTIR spectra and difference spectra [(tRNA solution + PEG solution) − (tRNA solution)] in the region of 1800−600 cm^{-1} for the free tRNA and free PEG 3350 (A), free PEG 6000 (B), and free mPEG-anthracene (C) and their complexes in aqueous solution at pH 7.3 with various polymer concentrations (0.125 and 1 mM) and constant tRNA content (12.5 mM).

reactive sites (major groove) and uracil O2 atom (minor groove). However, at 1 mM polymer concentration, reduction of intensity of the bases at 1698, 1660, and 1609 cm^{-1} was observed due to tRNA aggregation and particle formation (Figure 2A−C) consistent with our CD spectroscopic results and AFM imaging, which will be discussed in details further on.

PEG−Phosphate Binding. Strong PEG−PO_2 interaction was evident from an increase in the intensity and shifting of the PO_2 antiymmetric band at 1241 cm^{-1} [21,22,26−31] in the spectra of the polymer−tRNA complexes (Figure 1A−C). The PO_2 band at 1241 cm^{-1} gained intensity and shifted toward lower frequencies at 1235 (PEG 3350), 1237 (PEG 6000), and 1234 cm^{-1} (mPEG-anthracene) in the spectra of polymer−tRNA adducts (Figures 1 and 2A−C, complexes with 1 mM). The shifting of the phosphate band at 1241 cm^{-1} was associated with an increase in the intensity of this vibration upon polymer complexation (Figure 2A−C). Similar spectral changes were observed for the backbone PO_2 stretching vibrations in the IR spectra of dendrimer−tRNA, biogenic polyamine−tRNA, and cationic lipid−tRNA complexes, where strong ligand−phosphate binding occurred.[13,31,32]

Hydrophobic Contacts. A possible impact of PEG−tRNA interaction on polymer antisymmetric and symmetric CH_2 stretching vibration in the region of 3000−2800 cm^{-1} was investigated by infrared spectroscopy. The CH_2 bands of the free PEG 3350 located at 2944, 2883, and 2859 cm^{-1} shifted to 2886 and 2855 cm^{-1} (band 2944 did not shift) in PEG 3350-tRNA; free PEG 6000 with CH_2 bands at 2944, 2883, and 2859 cm^{-1} shifted to 2854 cm^{-1} (bands 2944 and 2883 did not shift)

dx.doi.org/10.1021/bm2016515 | Biomacromolecules 2012, 13, 282−287

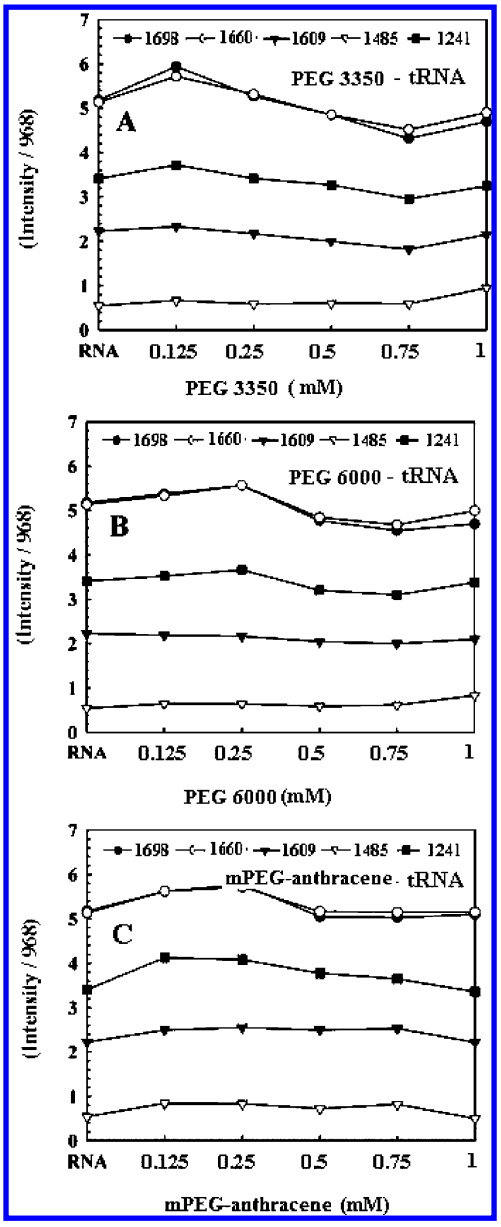

Figure 2. Intensity ratio variations of tRNA infrared in-plane vibrations upon polymer complexation for (A) PEG 3350-tRNA, (B) PEG 6000-tRNA, and (C) mPEG-anthracene-tRNA.

in PEG 6000-tRNA and free mPEG-anthracene with CH_2 bands at 2944, 2883, and 2857 cm^{-1} shifted to 2940 and 2886 cm^{-1} (2957 did not shift) in mPEG-anthracene-tRNA adducts (spectra not shown). The shifting of the polymer antisymmetric and symmetric CH_2 stretching vibrations, in the region 3000−2800 cm^{-1} of the infrared spectra, suggests the presence of hydrophobic interactions via polymer aliphatic chain and hydrophobic region in tRNA.

CD Spectra and tRNA Conformation. The CD spectra of tRNA and its complexes with different PEG concentrations are shown in Figure 3. The CD of the free tRNA is composed of four major peaks at 209 (negative), 221 (positive), 240 (negative), and 269 nm (positive) (Figure 3). This is consistent with CD spectra of double-helical RNA in A conformation.[33,34] At low PEG concentration (0.1 and 0.25 mM) no major shifting of CD bands was observed (Figure 3). As polymer concentration increased (0.5 and 1 mM), a major increase in

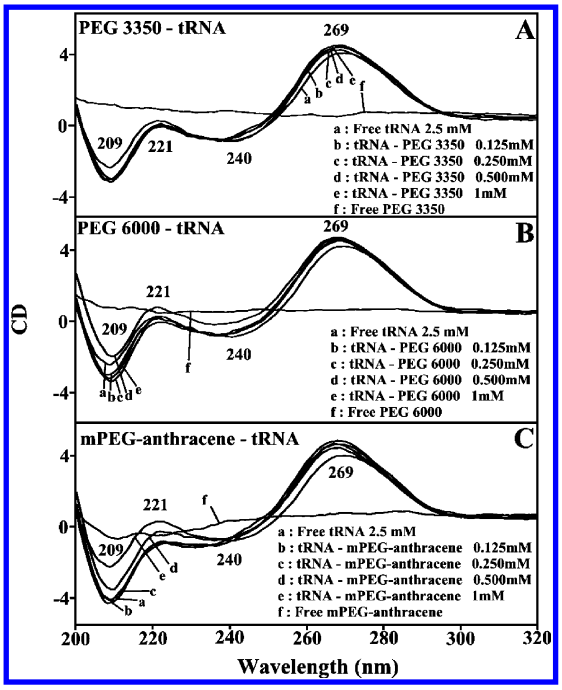

Figure 3. CD spectra of tRNA in Tris-HCl (pH ~7.3) at 25 °C (2.5 mM) and PEG 3350 (A), PEG 6000 (B), and mPEG-anthracene (C) with 0.125, 0.25, 0.5, and 1 mM polymer concentrations.

molar ellipticity of the band at 209 nm occurred and the amplitude of the band at 240 was reduced, whereas the intensity of the band at 269 decreased at high polymer concentration (Figure 3A−C). However, no major shifting was observed for the band at 269 nm in the spectra of polymer-tRNA complexes (Figure 3). This is due to the presence of tRNA in A-conformation both in the free state and in the polymer−RNA complexes. This is also consistent with the infrared results, which showed free tRNA in A-conformation with IR marker bands at 1698 (G), 1241 (PO_2), and 864 and 810 cm^{-1} (ribose-phosphate) with no major shifting of these bands in the polymer−tRNA complexes (Figure 1).

The reduced intensity of the band at 269 nm, in the spectra of PEG-tRNA together with the major intensity changes of the band at 209 and 221 nm, is due to the aggregation and particle formation of tRNA in the presence of PEG and mPEG-anthracene (Figure 3A−C). This is consistent with AFM imaging results of the PEG-tRNA complexes that showed tRNA aggregation and particle formation that will be discussed further on.

Stability of PEG-tRNA Complexes. The PEG-tRNA binding constant was determined as described in the Experimental Section (UV−visible spectroscopy). An increasing polymer concentration resulted into an increase in UV light absorption and of tRNA band at 260 nm (Figure 4). This is consistent with a reduction of base stacking interaction due to polymer complexation (Figure 4A−C). The double reciprocal plot of $1/(A - A_0)$ versus 1/(polymer concentration) is linear, and the binding constant (K) can be estimated from the ratio of the intercept to the slope (Figure 4A′,B′,C′). A_0 is the initial absorbance of the free tRNA at 260 nm, and A is the recorded absorbance of complexes at different polymer concentrations. The overall binding constant for PEG−tRNA complexes is estimated to be $K_{\text{PEG 3350-tRNA}} = 1.9\ (\pm 0.5) \times 10^4\ M^{-1}$, $K_{\text{PEG 6000-tRNA}} = 8.9\ (\pm 1) \times 10^4\ M^{-1}$, and $K_{\text{mPEG-anthracene}} = 1.2\ (\pm 0.40) \times 10^3\ M^{-1}$; stronger polymer−RNA complexation by PEG 6000 and PEG

dx.doi.org/10.1021/bm2016515 | Biomacromolecules 2012, 13, 282−287

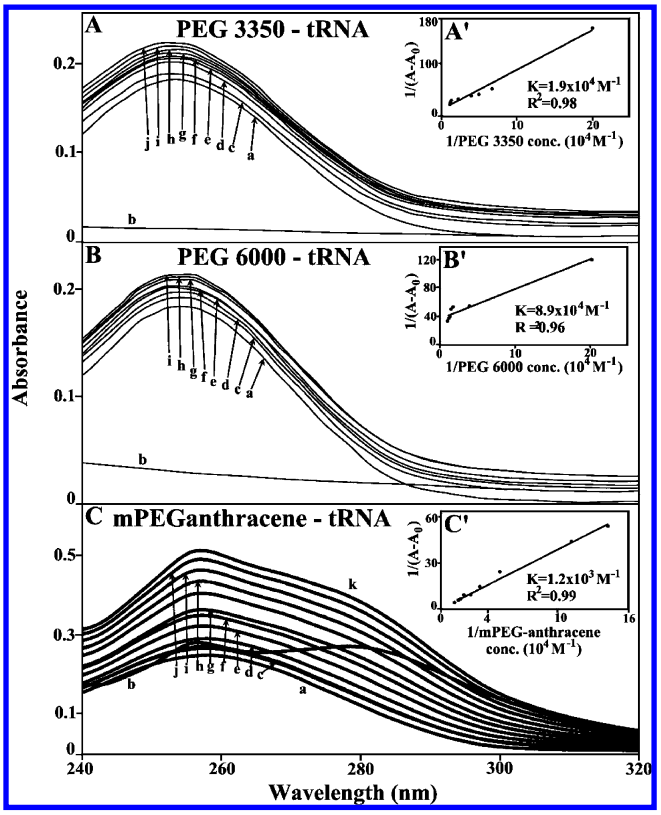

Figure 4. UV–visible results of tRNA and its PEG 3350 (A), PEG 6000 (B), and mPEG-anthracene (C) complexes: (A) spectra of (a) free tRNA (40 μM), (b) free PEG 3350 (100 μM), and (c–j) PEG 3350-tRNA complexes c (5), d (10), e (15), f (20), g (25), h (30), i (35), j (40), k (50), and l (60). (B) Spectra of (a) free tRNA (40 μM), (b) free PEG 6000 (100 μM), and (c–i) PEG 6000-tRNA complexes c (5), d (10), e (15), f (20), g (25), h (30), and i (35). (C) Spectra of (a) free tRNA (40 μM), (b) free mPEG-anthracene (100 μM), and (c–j) mPEG-anthracene-tRNA complexes c (5), d (10), e (20), f (30), g (40), h (50), i (60), and j (70). Plot of $1/(A - A_0)$ versus (1/polymer concentration) for K calculation of polymer and tRNA complexes, where A_0 is the initial absorbance of tRNA (260 nm) and A is the recorded absorbance (260 nm) at different polymer concentrations (5 to 80 μM) with constant tRNA concentration of 100 μM at pH 7.4 for PEG 3350 (A′), PEG 6000 (B′), and mPEG-anthracene (C′).

3350 than mPEG-anthracene is shown (Figure 4A′,B′,C′). The estimated binding constants are mainly due to the polymer–base binding, and they are not related to the polymer–PO_2 interaction, which is largely ionic and can be dissociated easily in aqueous solution.

Fluorescence Spectra and Stability of mPEG-anthracene-tRNA Adduct. Because tRNA is a weak fluorophore, the titration of mPEG-anthracene was done against various tRNA concentrations using mPEG-anthracene excitation at 330–350 nm and emission at 400–450 nm.[24] When mPEG-anthracene interacts with tRNA, fluorescence may change depending on the impact of such interaction on the mPEG-anthracene conformation or via direct quenching effect. The decrease in fluorescence intensity of mPEG-anthracene has been monitored at 420 nm for mPEG–anthracence–RNA systems. The plot of $F_0/(F_0 - F)$ versus 1/[tRNA] is shown in Figure 5A. Assuming that the observed changes in fluorescence come from the interaction between mPEG-anthracene and polynucleotides, the quenching constant can be taken as the binding constant of the complex formation. The K value given here is

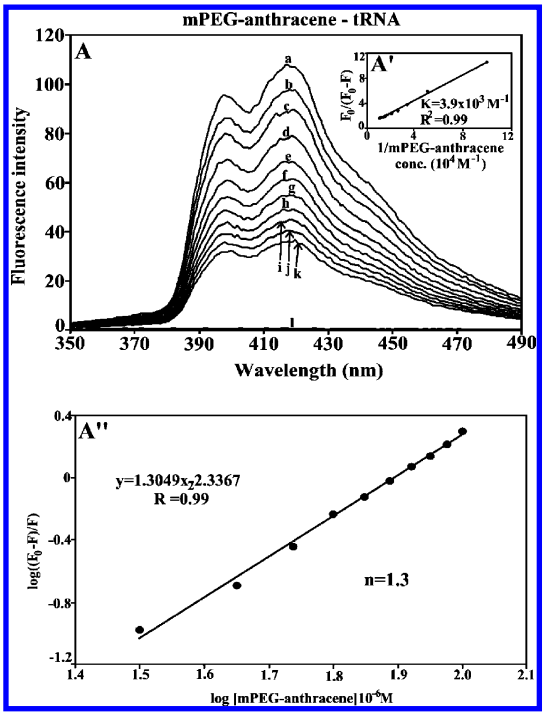

Figure 5. Fluorescence emission spectra of mPEG-anthracene-tRNA systems in 10 mM Tris-HCl buffer pH 7.4 at 25 °C for (A) polymer-DNA: (a) free mPEG-anthracene (80 μM) and (b–k) with polymer-RNA complexes at 5, 10, 15, 20, 30, 40, 60, 80, and 100 μM with (l) free tRNA 100 μM. The plot of $F_0/(F_0 - F)$ as a function of 1/tRNA concentration. The binding constant K is the ratio of the intercept and the slope for (A′) mPEG-anthracene-tRNA. (A″) The plot of log $(F_0 - F)/F$ as a function of log[tRNA] for calculation of the number of bound mPEG-anthracene molecules per tRNA (n) in polymer–RNA complexes.

the average of the four-replicate and six-replicate runs for mPEG-anthracene-tRNA systems, each run involving several different concentrations of tRNA (Figure 5A). The binding constant obtained was $K_{\text{mPEG-anthracene-DNA}} = 8.2\ (\pm 1) \times 10^3\ \text{M}^{-1}$ (Figure 4A′). The association constant calculated for the mPEG-anthracene-RNA adduct suggests low affinity mPEG-anthracene–polynucleotide binding. The f values obtained in Figure 5 suggest that tRNA also interacts with fluorophore via hydrophobic interactions, which is consistent with our infrared spectroscopic results discussed above (hydrophobic contacts).

The number of mPEG-anthracene molecules bound per polynucleotides (n) is calculated from log $[(F_0 - F)/F]$ = log $K_S + n$ log [tRNA] for the static quenching.[25,35,36] The linear plot of log $[(F_0 - F]/F]$ as a function of log [RNA] is shown in Figure 5A″. The n values from the slope of the straight line 1.3 for mPEG-anthracene-tRNA adduct (Figure 5A″). It seems that about one molecule of the PEG and mPEG-anthracene can bind tRNA tightly in these polymer–tRNA complexes.

Ultrastructure of PEG-tRNA Complexes. In all three cases, the mica surface was covered by small complexes (Figure 6) of various shapes. In each case, we were able to estimate the average height and average volume of the complexes. The PEG 3350 complexes had an average height of 0.75 ± 0.12 nm (n = 143) and an average volume of 61 nm^3 (Figure 6A). PEG 6000 complexes were doubled in height compared with the PEG 3350 ones, average height of 1.3 ± 0.3 nm (n = 208), and average volume of 520 nm^3 (Figure 6B). Finally, mPEG-anthracene complexes had an average height of 0.59 ± 0.2 nm (n = 108) and an average volume of 252 nm^3 (Figure 6C).

dx.doi.org/10.1021/bm2016515 | Biomacromolecules 2012, 13, 282–287

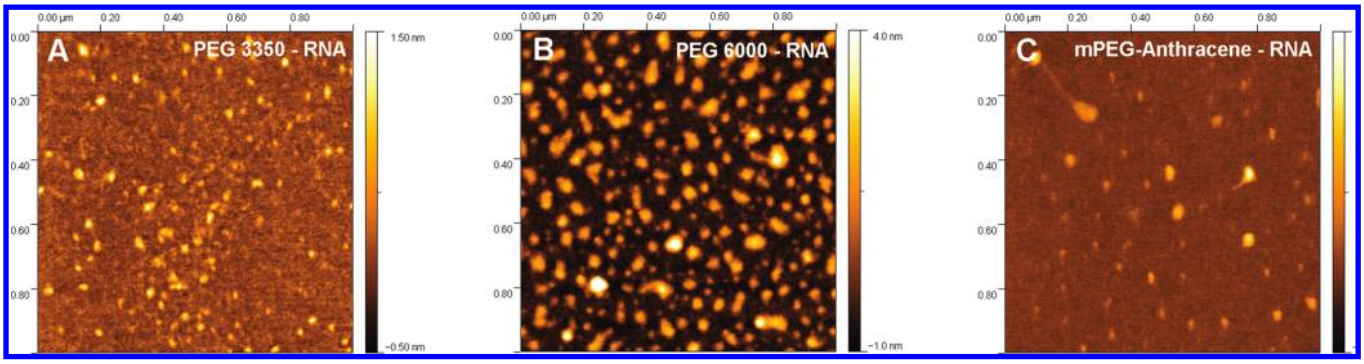

Figure 6. Tapping mode AFM pictures in air of PEG-tRNA complexes diluted 10 or 100 times in ultrapure water and adsorbed to mica. In all three cases, the surface was covered with aggregates. (A) Complexes with PEG 3350. (B) Complexes with PEG 6000. (C) Complexes with mPEG-anthracene.

Assuming a molecular weight of 27 kDa and a density of 1 g/cm^3, each tRNA molecule should occupy a volume of 45 nm^3. Therefore, the PEG 3350 complexes contain on average one tRNA molecule, the anthracene complexes contain five molecules, and the PEG 6600 complexes contain ten molecules. The tRNA aggregation and particle formation in the presence of PEG and mPEG-anthracene are very similar to those of PEG−DNA complexes recently reported.[37]

AUTHOR INFORMATION

Corresponding Author

*Tel: 819-376-5011 (ext. 3310). Fax: 819-376-5084. E-mail: tajmirri@uqtr.ca.

ACKNOWLEDGMENTS

This work is supported by grants from Natural Sciences and Engineering Research Council of Canada (NSERC).

ABBREVIATIONS:

PEG, poly(ethylene glycol); mPEG, methoxypoly (ethylene glycol); PAMAM, poly(amidoamine); A, adenine; G, guanine; C, cytosine; T, thymine; U, uracil; CD, circular dichroism; FTIR, Fourier transform infrared; AFM, atomic force microscopy

REFERENCES

(1) Svenson, S.; Donald A. Tomalia, D. A. *Adv. Drug Delivery Rev.* **2005**, *57*, 2106−2129.
(2) Wolinsky, J. B.; Grinstaff, M. W. *Adv. Drug Delivery Rev.* **2008**, *60*, 1037−1055.
(3) Yuan, Q.; Yeudall, W. A.; Yang, H. *Biomacromolecules* **2010**, *11*, 1940−1947.
(4) Kojima, C.; Kono, K.; Maruyama, K.; Takagishi, T. *Bioconjugate Chem.* **2000**, *11*, 910−917.
(5) Fant, K.; Esbjorner, E. K.; Jenkins, A.; Grossel, M. C.; Lincoln, P.; Norden, B. *Mol. Pharmaceutics* **2010**, *7*, 1743−1746.
(6) Bello-Roufai, M.; Lambert, O.; Pitard, B. *Nucleic Acids Res.* **2007**, *35*, 728−739.
(7) Wang, R.; Zhou, L.; Zhou, Y.; Li, G.; Zhu, X.; Gu, H.; Jiang, X.; Li, H.; Wu., J.; He, L.; Guo, X.; Zhu, B.; Yan, D. *Biomacromolecules* **2010**, *11*, 489−495.
(8) Casettari, L.; Vllasaliu, D.; Mantovani, G.; Howdle, S. M.; Stolnik, S.; Illum, L. *Biomacromolecules* **2010**, *11*, 2854−2865.
(9) Kim, W.; Yamasaki, Y.; Jang, W. D.; Kataoka, K. *Biomacromolecules* **2010**, *11*, 1180−1186.
(10) Wu, J.; Zhou, J.; Qu, F.; Bao, P.; Zhang, Y.; Peng, L. *Chem. Commun.* **2005**, 313−315.
(11) Jensen, L. B.; Mortensen, K.; Pavan, G. M; Kasimova, M. R.; Jensen, D. K.; Gadzhyeva, V.; Nielsen, H. M.; Foged, C. *Biomacromolecules* **2010**, *11*, 3571−3577.
(12) De Paula, D.; Vitoria, M.; Betley, L. B.; Mahato, R. I. *RNA* **2007**, *13*, 431−456.
(13) Froehlich, E.; Mandeville, J. F.; Weinert, C. M.; Kreplak, L.; Tajmir-Riahi, H. A. *Biomacromolecules* **2011**, *12*, 2780−2787.
(14) Froehlich, E.; Mandeville, J. F.; Weinert, C. M.; Kreplak, L.; Tajmir-Riahi, H. A. *Biomacromolecules* **2011**, *12*, 511−517.
(15) Froehlich, E.; Jennings, C. J.; Sedaghat-Herati, M. R.; Tajmir-Riahi. *J. Phys. Chem. B* **2009**, *113*, 6986−6993.
(16) Mandeville, J. S.; Tajmir-Riahi, H. A. *Biomacromolecules* **2010**, *11*, 465−472.
(17) Lakowicz, J. R. In *Principles of Fluorescence Spectroscopy*, 3rd ed.; Springer: New York, 2006.
(18) Marmur, J. J. *Mol. Biol.* **1961**, *3*, 208−218.
(19) Reichmann, M. E.; Rice, S. A.; Thomas, C. A.; Doty, P. *J. Am. Chem. Soc.* **1954**, *76*, 3047−3053.
(20) Vijayalakshmi, R.; Kanthimathi, M.; Subramanian, V. *Biochem. Biophys .Res. Commun.* **2000**, *271*, 731−734.
(21) Alex, S.; Dupuis, P. *Inorg. Chim. Acta* **1989**, *157*, 271−281.
(22) Ahmed Ouameur, A.; Tajmir-Riahi, H. A. *J. Biol. Chem.* **2004**, *279*, 42041−42054.
(23) Connors, K. *Binding Constants: The Measurement of Molecular Complex Stability*; John Wiley & Sons: New York, 1987.
(24) del Valle, J. C.; Turek, A. M.; Tarakalanov, N. D.; Saltiel, J. *J. Phys. Chem. A* **2002**, *106*, 5101−5104.
(25) Mandeville, J. S.; N'soukpoé-Kossi, C. N.; Neault, J. F.; Tajmir-Riahi, H. A. *Biochem. Cell Biol.* **2010**, *88*, 469−477.
(26) Andrushchenko, V. V.; Leonenko, Z.; van de Sande, H.; Wieser, H. *Biopolymers* **2002**, *61*, 243−260.
(27) Dovbeshko, G. I.; Chegel, V. I.; Gridina, N. Y.; Repnytska, O. P.; Shirshov, Y. M.; Tryndiak, V. P.; Todor, I. M.; Solyanik, G. I. *Biopolymers (Biospectroscopy)* **2002**, *67*, 470−486.
(28) Loprete, D. M.; Hartman, K. A. *Biochemistry* **1993**, *32*, 4077−4082.
(29) Taillandier, E.; Liquier, J. *Methods Enzymol.* **1992**, *211*, 307−335.
(30) Theophanides, T.; Tajmir-Riahi, H. A. *J. Biomol. Struct. Dyn.* **1985**, *2*, 995−1004.
(31) Ahmed Ouameur, A.; Bourassa, P.; Tajmir-Riahi, H. A. *RNA* **2010**, *16*, 1968−1979.
(32) Marty, R.; N' soukpoe-Kossi, C. N.; Charbonneau, D.; Weinert, C. M.; Kreplak, L.; Tajmir-Riahi, H. A. *Nucleic Acids Res.* **2009**, *37*, 5197−5207.
(33) Kypr, J.; Vorlickova, M. *Biopolymers (Biospectroscopy)* **2002**, *67*, 275−277.
(34) Vorlickova, M. *Biophys. J.* **1995**, *69*, 2033−2043.
(35) Charbonneau, D. M.; Tajmir-Riahi, H. A. *J. Phys. Chem. B* **2010**, *114*, 1148−1155.
(36) Mandeville, J. S.; Tajmir- Riahi, H. A. *Biomacromolecules* **2010**, *11*, 465−472.
(37) Froehlich, E.; Mandeville, J. F.; Arnold, D.; Kreplak, L.; Tajmir-Riahi, H. A. *J. Phys. Chem. B* **2011**, *115*, 9873−9879.